Silk fibroin nanofibers containing chondroitin sulfate and silver sulfadiazine for wound healing treatment

Marília Cestari, Bárbara Sthéfani Caldas, Pereira Fonseca, Rodolfo Bento Balbinot, Danielle Lazarin-Bidói, Issei Otsuka, Celso Vataru Nakamura, Redouane Borsali, Edvani Curti Muniz

PREPRINT

(Original article published in Journal of Drug Delivery Science and Technology 70 (2022) 103221 by Elsevier B.V., DOI: 10.1016/j.jddst.2022.103221)

Silk fibroin nanofibers containing chondroitin sulfate and silver sulfadiazine for wound healing treatment

Marília Cestari[a], Bárbara Sthéfani Caldas[a], Dyenefer Pereira Fonseca[b], Rodolfo Bento Balbinot[b], Danielle Lazarin-Bidói[a b], Issei Otsuka[c], Celso Vataru Nakamura[b], Redouane Borsali[c], Edvani Curti Muniz[a,d,e,*]

a. Department of Chemistry, State University of Maringá, Av. Colombo, 5790, 87020-900, Maringá, Brazil.
b. Department of Health Basic Science, State University of Maringá - UEM, 87020-900 Maringá, Brazil
c. CNRS, CERMAV, University of Grenoble Alpes, 38000 Grenoble, France
d. Federal University of Technology - Paraná, Estrada dos Pioneiros, 3131, CEP 86036-370, Londrina, Brazil.
e. Department of Chemistry, Federal University of Piauí, Campus Petrônio Portella, Ininga, Teresina, 64049-550, Piauí, Brazil.

** **Corresponding author:** *ecmuniz@uem.br*; *munizec@ufpi.edu.br*.

Abstract

Nanofibers containing silk fibroin (SF), chondroitin sulfate (CS) and silver sulfadiazine (SSD) were made up by electrospinning technique. Poly(ethylene oxide) (PEO) was added to the acidic water solution used for electrospinning to improve electrospinnability. Fibers were characterized by Scanning Electron Microscopy (SEM), Fourier transform infrared spectroscopy (FTIR-ATR), Energy Dispersive X-ray Spectroscopy (EDS), Differential Scanning Calorimetry (DSC) and biological analysis. The FTIR-ATR and DSC results showed that PEO was removed from the surface of the nanofibers by washing the as-spun fibers with absolute ethanol. FTIR-ATR and EDS results showed that CS and SSD remained in the nanofibers. Biological assays showed that the as-obtained nanofibers are not toxic to healthy Vero cells. Antibacterial activity tests showed that the concentration of CS significantly influenced the antibacterial activity of the samples. In vivo experiments with Wistar rats revealed that SF nanofibers containing CS and SSD had similar results to standard SSD cream treatment, with the advantage of being applied only once to the patient avoiding discomfort and pain in dressing changes. CS played an important role as a stabilizing agent of electrospinning solutions improving SSDremaining and enhancing the antibacterial activity of nanofibers against bacteria through in vitro.

Keywords: *electrospinning; biopolymers; nanomaterial; wound dressing; antibacterial activity; in vivo assays*

1.Introduction

Burn injuries are a serious problem. They are associated with a significant incidence of death and disability, various surgical procedures, prolonged hospitalization, and high health care costs [1]. Bacterial infection is one of the most frequent and serious complications in patients with burns, as it can delay the healing of wounds, increase scarring and favor the proliferation of microorganisms that can result in invasive infections and that can lead to the patient's death [2–4]. Wound dressings devices are an important segment of the worldwide medical and pharmaceutical field in the treatment of wounds. In the past, traditional dressings such as natural or synthetic bandages, cotton, lint, and gauze, all with varying degrees of absorption, have been used for wound management. The main functions of wound dressings devices was to keep the wound dry, allowing the exudates from the wound be adsorbed and/or to evaporate, preventing odors and harmful bacteria from entering the wound [5], to enable rapid healing [6], to reduce pain, to keep the moisture [7]. An open wound is a favorable niche for microbial colonization [8]. Generally, most of infected wounds have polymicrobial and are, generally, contaminated by pathogens found in the vicinity of the environment, that are endogenous microbe (that live in the membrane's mucous) and also by the microflora available in the adjacent skin [9]. In the early stages of the formation of chronic wounds, gram-positive organisms, specifically S. aureus, are predominant [10]. In the later stages, on the other hand, gramnegative species such as E. coli and P. aeruginosa are observed and tend to invade deeper layers of the skin causing significant tissue damage [10]. Nowadays, bacterial contamination of skin wounds is responsible for high rates of morbidity and mortality [11]. Therefore, different laboratories around the world have started to develop antimicrobial dressings to prevent contamination of the wound [12]. Different materials had been used in developed dressings and various physical forms (sponges, hydrogels, hydrocolloids, films, membranes, etc.) had been proposed. The different formulations have distinct properties that make them suitable for the treatment of a certain types of wounds. Synthetic and/or natural polymers, which are biocompatible and/or biodegradable, can be used as raw materials to produce skin and wound dressings to treat burns and chronic non-healing wounds. Their compatibility and characteristics enable cell proliferation, protection to the tissues and fast recovery [6,7]. Nanofibers are known to act as physical barriers, as well as to reproduce the 3D architecture of the native extra cellular matrix (ECM). Also, nano/microfibers provide the desired properties for dressings, such as exudate absorption, oxygen permeability [13–15], and yet, their high surface-volume ratio and interconnected pores are crucial to ensure cell proliferation, gas exchange, supply of nutrients and control fluid loss [13]. The main disadvantages associated with the use of nanofibers are caused by the materials and solvents used in their production [16,17]. Nanofibers can be manufactured using electrospinning method due to their versatility to produce fibers with structure, porosity, orientation, morphology, and dimension control.

To improve the antimicrobial properties of the dressing, different agents can be incorporated into its structure. Antimicrobial agents essentially comprise antibiotics (for example, tetracycline, ciprofloxacin, gentamicin, and sulfadiazine), nanoparticles (for example, silver nanoparticles), and natural products (for example, honey, essential oils, and chitosan) [9]. Silver sulfadiazine (SSD) is widely used as an effective antibiotic for burn injuries. Besides, SSD is used against bacterial activity in the treatment of infected wounds [18] and also effective against super-resistant bacteria [19]. However, it has been shown that SSD can be cytotoxic. Therefore, it is important to reduce the risk of cytotoxicity, reducing the amount of SSD added to the dressing as well as controlling the release of Ag^+ through the vehicle used [20]. Many synthetic and natural polymers have been studied to manufacture dressings. Among them, silk fibroin (SF) stands out for being a natural biopolymer, present in the shell of cocoons produced by the Bombyx mori species [21]. Bombyx mori silk is composed of two main proteins: fibroin and sericin. SF is the main constituent of cocoons manufactured by silkworms. Sericin, on the other

hand, coats SF, acts as an adhesive, and is present in a smaller quantity [22]. SF properties such as slow biodegradation, excellent mechanical properties, favorable processability in conjunction with biocompatibility, are responsible for the great interest in this material for a variety of applications, from the textile area to biomedical use [23]. Jeong, L. et al [24] have studied the wound healing effect of SF nanofibrous matrices containing silver sulfadiazine (SSD) and they reported cytotoxic effects in normal human epidermal keratinocytes (NHEK) and normal human epidermal fibroblasts (NHEF).

In the face of these results, a similar system (nanofibers of SF/SSD) was studied and chondroitin sulfate (CS), a polymer widely used in biomaterials, was used to enrich the formulation developed in present work. CS is a biopolymer belonging to the class of glycosaminoglycans, GAGs, and a structural component of the cartilaginous matrix [18]. The high negative polarity resulting from -SO4-2 and -COO- groups present on CS make possible this polymer be used as polyanion, on which positively charged growth factors can be adsorbed and enriched to induce adhesion, differentiation, and migration cell [25]. It is evident that CS plays important role in the wound healing process. Gilbert et al. (2004) [26] found that CS's hydrogel accelerates the healing of wounds in the nasosinusal mucosa in a final period of 4 days. This finding suggests that SC has the potential to improve wound healing and also can maintain an adequate microenvironment for cell growth [25]. Zou et al. (2009) [27] studied the interaction between SC and human fibroblasts in wound healing. The results of this study demonstrated that: (i) the SC regulates cell adhesion and proliferation, as well as the cell cycle; and (ii) the SC modulates the wound closure and contraction rate in vitro. Also, they found that CS promotes cell proliferation. These results showed that CS is extremely important for cell division. In addition to these findings, the data also showed that CS is involved in the division and proliferation of human cells. In summary, CS has crucial biological functions in cellular activities and great potential as a biomaterial for tissue engineering and wound repair. Thus, the evaluated hypothesis in this work remains in the union of the excellent characteristics of these two biopolymers (SF and CS) with the antimicrobial action of SSD can produce new dressings with the potential to control the wound infections. Besides, the new dressings would improve the progress of the organized stages of healing and would present cytocompatibility, which can be an advance on currently available strategies.

2.Material and Methods

2.1 Material

Vale da Seda Institute (Maringá-PR, Brazil) kindly supplied the silkworm cocoons of Bombyx mori. Solabia Biotecnológica Ltda. (Maringá-PR, Brazil) kindly supplied the chondroitin sulfate and Prati-Donaduzzi Medicamentos Genéricos (Toledo-PR, Brazil) furnished the silver sulfadiazine (SSD). The other used chemicals, such as ethanol, sodium bicarbonate, calcium chloride, and PEO (Mw = 900 kDa) were purchased from Sigma-Aldrich (Darmstadt, Germany). Exception for the silkworm cocoons, all other reagents were used as received, without prior purification.

2.2 Methods

Raw silk fibers were degummed twice with 0.5% (w/w) NaHCO3 solution at 100 oC for 30 min and then washed three times against distilled water at 70 °C to remove the sericin. The degummed fibroin was dissolved in ethanol/water 20/80 (v/v) CaCl2 containing 5 mol L-1 at 80 °C until complete dissolution (about 30 min). Then, the fibroin solution was dialyzed for three days in a cellulose acetate membrane against distilled water [23,24]. After that, the dialyzed solution was filtered to remove impurities and the final concentration was determined by the residual solid weight of a known volume, after drying at 60 °C for 24 h [30].

2.2.1 Preparation of electrospinning solutions.

SSD was dispersed in 1.2 mL of distilled water/HCl at pH = 1.0 (obtained by adding HCl 1.0 mol L^{-1}) for 0.1%, 0.5% and 1.0% (w/v) SSD concentrations, relative to the solution final volume (4 mL). After, the solution was sonicated for 90 min. Then, CS [at 1.0%, 3.0% and 5.0% (w/v) concentrations, relative to the solution final volume (4 mL)] and PEO [at 7.5% (w/v), relative to the solution initial volume (1.2 mL)] were added to the solution and stirred for 24 h. After that, 2.8 mL of SF aqueous solution 8.5 % (m/v) were added to the previous solution (containing SSD, PEO and CS), see Table 1, and the resulting solution (4 mL) was maintained under stirring in ice bath for 1 hour, until the obtainment of the electrospinning solution [26,30].

Table 1
SSD and CS concentrations used in nanofibers fabrication.

Sample	Conc. SSD (w/v-%)	Conc. CS (w/w-%)
1	1.00	5.00
2	1.00	1.00
3	0.10	5.00
4	0.10	1.00
5	0.55	3.00

2.2.2 Preparation of SF/PEO/CS/SSD scaffolds
Nanofibers were obtained through electrospinning process using an Esprayer ES- 2000S2A (Fuence Co., Ltd., Tokyo, Japan) equipment. To produce homogeneous nanofibers the parameters of electrospinning were fixed at 20 kV of voltage; 17 cm of distance capillary-collector; and 8.5 μL min-1 of solution flow. Humidity varied between 33 - 61% and temperature varied between 26 – 31 °C during the process. At the end of the process, the nanofibers were immersed in absolute ethanol for 3 days at 60 °C (ethanol was replaced every 24 h) to remove PEO. Then the nanofibers were dried at room temperature for 24 h.
2.2.3 Characterization of SF/PEO/CS/SSD scaffolds.
2.2.3.1) Through scanning electron microscopy (SEM)
After being coated with gold, the nanofibers were morphologically analyzed through scanning electron microscopy (SEM) using an equipment QUANTA FEG 250 (FEI Co., Hillsboro,

U.S.A.). The average diameter for each type of fiber was calculated with the SIZE METER® software, version 1.1.

2.2.3.2) Through Fourier transform infrared spectroscopy with attenuated total reflectance (FTIR-ATR)

The spectra were obtained on a Perkin Elmer FTIR machine with ATR apparatus, model RXI FTIR, operating in the 4000-400 cm-1 range, with a resolution of 4 cm-1. Each FTIR spectrum was obtained using 4 scans.

2.2.3.3) Through differential scanning calorimetry (DSC)

The equipment TA Instrument, model Q20, was used to obtain the DSC curves of the nanofibers. For each analysis, about 7.0 mg of nanofibers were used in an aluminum pan. The temperature range was 25 to 150 °C at a rate of 10 °C min-1, in a 50 mL min-1 N2 atmosphere.

2.2.3.4) Through X-ray energy dispersive spectroscopy (EDS)

After being coated with thin carbon film, the nanofibers were analyzed by an Xray photoelectron spectrometer using a detector SDD (BRUKER AXS-30 mm^2) coupled to an equipment FEG ZEISS Ultra 55.

2.2.3.5) Through flame atomic absorption spectroscopy (FAAS)

After nanofibers being washed with ethanol, the remained amount of SSD was determined by FAAS (Varian, model AA 240FS – Fast Sequential Atomic Absorption Spectrometer) with a silver hollow cathode lamp operating at 5 mA. The measurement wavelength was 328.1 nm. Acid digestion of all samples (about 10 mg) was carried out using 10 mL of nitric acid 65% (v/v), in which the solution was heated until about 1 mL. After dilution with Milli-Q® water by 50 or 25 folds, depending on the sample. An analytical curve was built using a standard Ag+ aqueous solution (1 g L-1) diluted to achieve concentration range of 0.25 mg L-1 to 10 mg L-1. The amount of SSD by weight of nanofibers (WSSD, in mg g-1) was obtained by the following equation:

$$WSSD = [CAg \times Vsol/(MAg/MSSD)] \times (1/Wsample)$$

Where CAg is the Ag concentration at the measured solution by FAAS (μg mL-1), Vsol is the solution volume (mL), MAg and MSSD are the atomic mass of Ag and SSD, respectively, in g mol-1; and Wsample is the weight of the analyzed nanofibers (mg). The experiment was carried out in duplicate.

2.2.4 Biological assays

2.2.4.1) Through cytotoxicity on mammalian cells

This test was performed to evaluate the influence of the SF/PEO/CS/SSD scaffolds on the cell viability of mammalian cells. To this end, Vero cells (epithelial kidney cells of Cercopithecus aethiops) cultivated in DMEM (Dulbecco's Modified Eagle Medium, Gibco® Invitrogen) supplemented with 2 mM L^{-1} glutamine and 10 % fetal bovine serum (FBS) was obtained, quantified, and seeded into 24-well culture plates at a concentration of 2.5 x 105 cells mL^{-1}, and kept in a moist chamber at 37 °C and a 5% CO_2 atmosphere. After elapsed 24 h of incubation serum-free DMEM, discs (6 mm of diameter) of the SF/PEO/CS/SSD scaffolds were added, proceeding incubation for 72 h and replaced the culture medium. At the end of the incubation, the cell growth was determined by the method of reduction of MTT viability [35]. This colorimetric method is based on the ability of mitochondria of viable cells to reduce MTT (tetrazolium salt) into a compound purple insoluble called formazan. For this, the cells were washed thoroughly with phosphate-buffered saline (PBS) and incubated in 250 μL of MTT solution (2 mg mL^{-1}) under absence light at 37 °C. After 4 h of incubation, 750 μL of dimethylsulfoxide was added to each well to solubilize the formazan crystals and the spectrophotometric reading was performed at λ = 570 nm in a microplate reader (Bio Tek - Power Wave XS, USA). Cells cultured in the absence of the silk fibroin nanofibers were used as control and taken as 100 % growth. The results were expressed as a percentage of cytotoxicity, by the following equation:

(%) = (A_s – A_c) x 100
where *As* and *Ac* are the absorbance of the test sample and negative control, respectively.

2.2.4.2) Through antibacterial activity

Escherichia coli ATCC 25922, *Pseudomonas aeruginosa* ATCC 27853, *Bacillus subtilis* ATCC 6623 and *Staphylococcus aureus* ATCC 25923 were the microorganisms used at the tests. They were cultivated in Mueller broth Hinton (Difco) a 37 °C for 24 h. For the tests, cellular density was standardized in tubes containing saline solution 0.9 % sterile, that the turbidity was identical to the McFarland scale tube which corresponds to 1 x 10^8 CFU mL^{-1} [36]. The diffusion halo test was realized in agar Muller-Hinton media. The bacteria were suspended in saline solution e seeded on the agar plate. After, the nanofibers discs were placed. The plates were incubated at 37 °C for 24 h. After this period, the diameters of the inhibition halos formed around the discs were measured and the results expressed in millimeters [37]. The experiments were performed in triplicate (n = 3).

2.2.4.3) Through biological activity *in vivo* evaluation

Male Wistar rats (isogenic) with 7 weeks old (200-250 g) were obtained in the central vivarium at the State University of Maringá (UEM, Maringá-Brazil). They were set in the vivarium of the Laboratory of Technological Innovation in the Development of Pharmaceuticals and Cosmetics, at the UEM, for seven days before being experimentally infected. The animals were kept in individual cages. The room temperature was maintained at 22 ± 2 °C and humidity at 45 to 55% in a 12 h light/dark cycle. The animals were fed ration and water *ad libitum*. This project was duly submitted for approval by the Committee of Ethical Conduct in the Use of Animals in Experiments (CEAE) at the State University of Maringá to perform the *in vivo* experiments (No. 9326060618/2018).

The bacteria *S. aureus* ATCC 25923 and *P. aeruginosa* ATCC 27853 were cultured in Mueller Hinton Broth (CMH) (Difco) at 37 °C.

For biological activity *in vivo* evaluation of SF nanofibers containing chondroitin sulfate and silver sulfadiazine in Wistar rats infected with *S. aureus* and *P. aeruginosa*, the animals were divided into 9 groups, each group containing 5 animals: (G1) uninfected and untreated; (G2) infected with *S. aureus* and untreated; (G3) infected with *P. aeruginosa* and untreated; (G4) infected with *S. aureus* and treated with silver cream sulfadiazine (1.0%) topically; (G5) infected with *P. aeruginosa* and treated with silver cream sulfadiazine (1.0%) topically; (G6) infected with *S. aureus* and treated with SF nanofibers topically; (G7) infected with *P. aeruginosa* and treated with SF nanofibers topically; (G8) infected with *S. aureus* and treated with SF nanofibers containing chondroitin sulfate (3.0%) and silver sulfadiazine (0.55%) topically; (G9) infected with *P. aeruginosa* and treated with SF nanofibers containing chondroitin sulfate (3.0%) and silver sulfadiazine (0.55%) topically. For this, Wistar rats were anesthetized with sodium thiopental (50 mg Kg^{-1}) and lidocaine (10 mg Kg^{-1}), and the dorsal hairs were carefully removed. After 2 days, the animals were anesthetized, and a skin wound was surgically performed on the back with a 6 mm biopsy puncture. Infection at the wound site was then performed by adding 10 μL of a 1 x 10^8 CFU mL^{-1} solution of *S. aureus* or *P. aeruginosa*. Treatment was started 72 h after topical infection and then covered with Tegaderm® to keep the nanofibers in place. Wounds from control groups (G1, G2, and G3) were covered with Tegaderm® only. Animals from groups G4 and G5 were treated daily. Treatment was evaluated after 5 days. The animals were euthanized using an intraperitoneal injection of sodium thiopental and lidocaine solution, followed by cervical dislocation. The skin was removed, washed, and submitted to histopathological analysis. Additionally, the animals were weighed throughout the experiment.

For analysis histopathological of the skin, after removal and washing in PBS

buffer, the animals' skin was fixed in Bouin's solution (saturated aqueous picric acid, formaldehyde, and acetic acid), dehydrated in ethanol (70%, 80%, 90%, and 100%) and, lastly, in xylol for 12 h at least. Xylol was gradually substituted by paraffin at 70 °C, until the complete inclusion. Sections of 6 μm were obtained using a microtome (Leica Microsystems Inc., Germany), collected in slides previously prepared with poly-L-lysine, stained in Harris' hematoxylin-yellow eosin, and mounted using Permount™ mounting Medium. The sections were analyzed under an Olympus CX31 microscope (Olympus, Tokyo, Japan), and the images were captured on an Olympus SC30 camera (Olympus, Tokyo, Japan).

3. Results and discussion

3.1 Electrospinning and characterization of the nanofibers

3.1.1 Scanning electron microscopy (SEM).

SF/CS/SSD nanofibers were successfully fabricated from aqueous solutions at pH = 1.0. As can be observed in SEM images of Figure 1, the nanofibers are homogenous, without beads, before and after PEO removal. The average diameter of nanofibers is shown in Table 2. Changes in the morphology of the nanofibers after the removal of PEO was observed in all samples, where they showed a flattening and some points where the fibers adhered to each other. These changes were more evident in samples 3.1 and 5.1, the only samples where the PEO was completely removed (as indicated by DSC analysis). The average diameter of nanofibers before and after the removal of PEO is shown in Figure 2. No significant variation was verified in the diameters due to the process of removal of PEO by washing with absolute ethanol. This may have occurred due to the flattening of the nanofibers, which meant that no significant change in the diameter occurred, but there may have been change in the thickness of the nanofibers if they assumed ribbon morphology. Besides, the low diameter of the fibers represents bigger surface area in a small space, which enables healthy cells to attach and proliferate and favors the availability of the Ag^{2+} active principle. Mina Mohseni et al. work [38], showed that PVA/SSD fibers presented an enlargement behavior as the amount of SSD was augmented, which may not be interesting considering tissue regeneration.

Table 2
Concentrations of CS and SSD, relative humidity, temperature, and average diameter of nanofibers, before* and after** the PEO removal.

Sample	Conc. SSD (%)	Conc. CS (%)	Humidity (%)	Temp. (°C)	Nanofibers average diameter (nm)
1*	1.0	5.0	61.2	26.1	324 ± 44
1.1**					345 ± 75
2*	1.0	1.0	47.0	27.3	297 ± 41
2.1**					255 ± 32
3*	0.1	5.0	44.2	25.1	328 ± 43
3.1**					334 ± 53
4*	0.1	1.0	42.0	27.3	262 ± 39
4.1**					242 ± 32
5*	0.5	3.0	41.3	25.4	294 ± 36
5.1**					271 ± 38

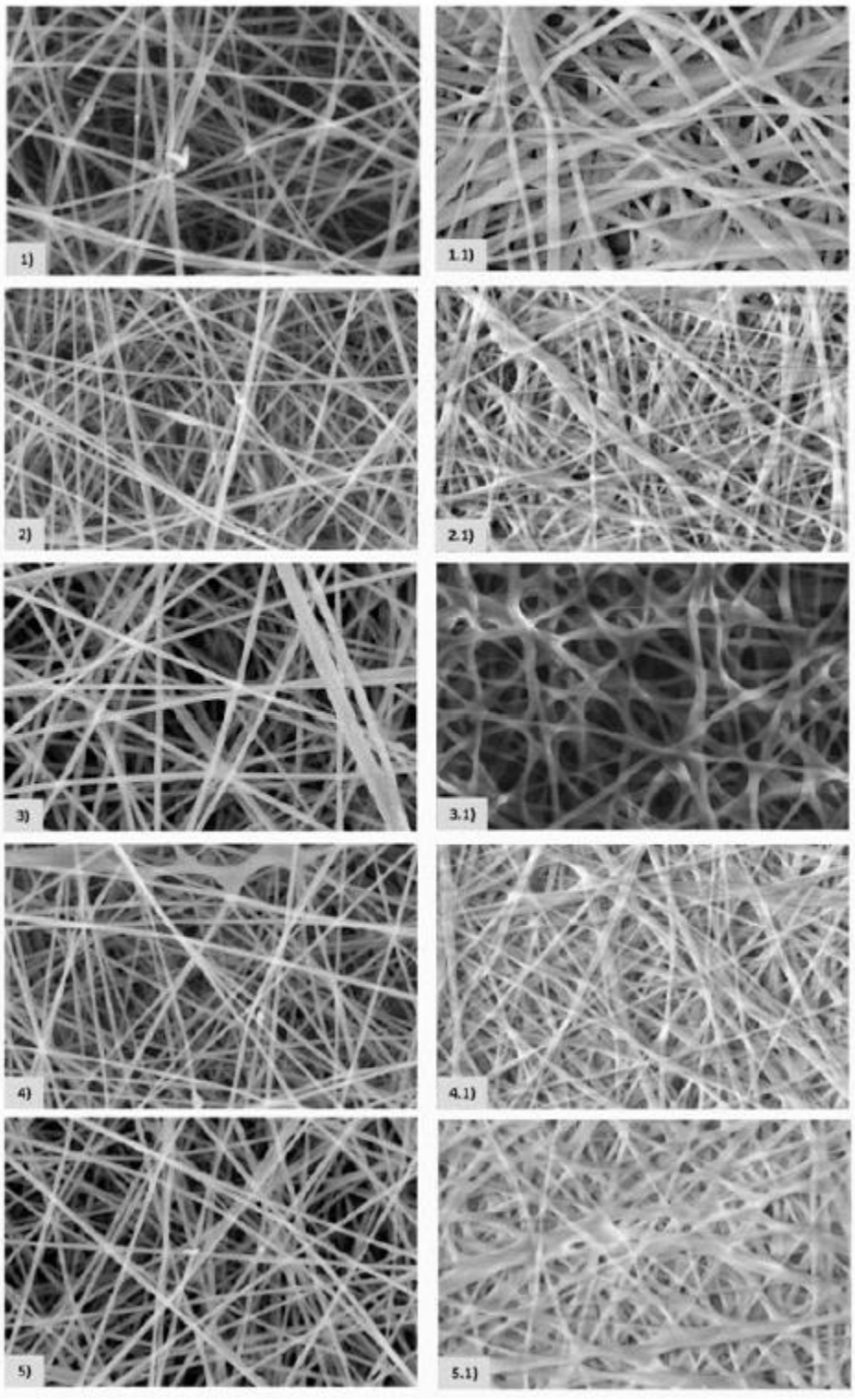

Figure 1

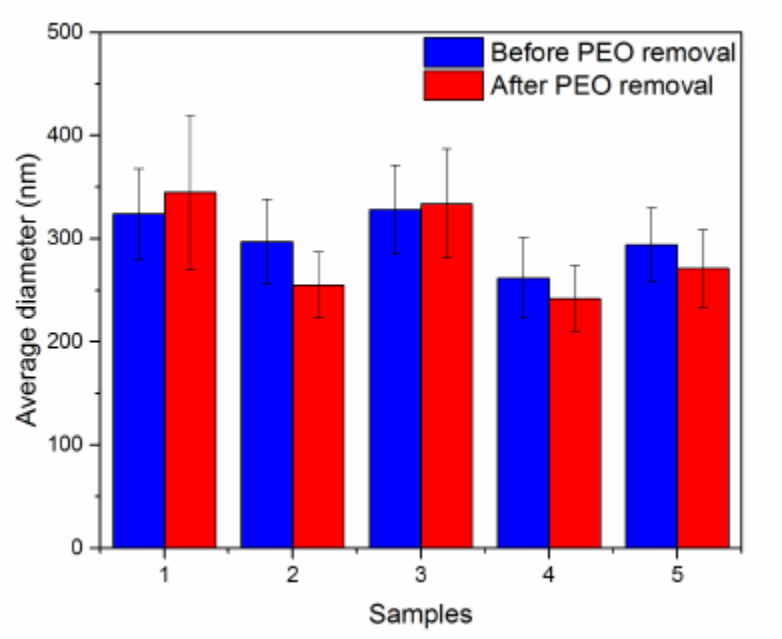

Figure 2

3.1.2 Fourier transform infrared spectroscopy (FTIR).

FTIR-ATR analysis is commonly used for investigating SF structure because the position of amide bands is very sensitive to conformation changes [33,34]. Furthermore, this technique was used to evaluate the SF structure, the PEO removal, and to characterize possible interactions between SF and other materials (CS and SSD). **Figure 3** displays the FTIR spectra of nanofibers, in which characteristic bands of SF amide I and amide II shifted to lower wavenumbers after the fibers being washed with absolute ethanol (samples 1.1, 2.1, 3.1, 4.1, and 5.1). These shifts (from 1648 cm^{-1} to 1625 cm^{-1} for amide I; and from 1530 cm^{-1} to 1517 cm^{-1} for amide II) can be attributed to the change in SF conformation from random coil to β-sheet [40], once SF macromolecules can rearrange their crystal structure due to changes in hydrogen bonding caused by physical contact such as immersion of the nanofibers in ethanol [39].

PEO characteristic bands disappeared at 2874 cm^{-1} and at 1100 cm^{-1} after washing the nanofibers with absolute ethanol, indicating that PEO has been removed from the fibers' surface. The presence of the band at 1030 cm^{-1}, attributed to CS, indicates that even after washing with absolute ethanol, the CS remained in the nanofibers, as expected because the CS is highly soluble in water but not in absolute ethanol [41].

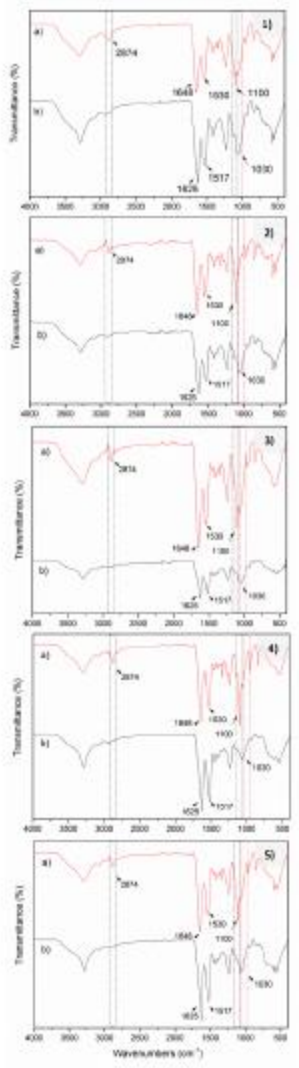

Figure 3

3.1.3 Differential scanning calorimetry (DSC).

Figure 4 shows the DSC curves of nanofibers obtained under various conditions.
An endothermic peak close to 60 °C due to PEO fusion confirms the presence of PEO in the SF/PEO nanofibers (used as control). The presence of this endothermic peak was not observed in samples 3.1 and 5.1, indicating that in these samples the PEO was completely removed through fibers exposure to absolute ethanol. These samples also showed a more evident change in morphology when compared to the others observed by SEM analysis. The other samples showed an endothermic peak close to 60 °C indicating that PEO was removed only from the surface of the nanofibers, as demonstrated by FTIR-ATR analysis.

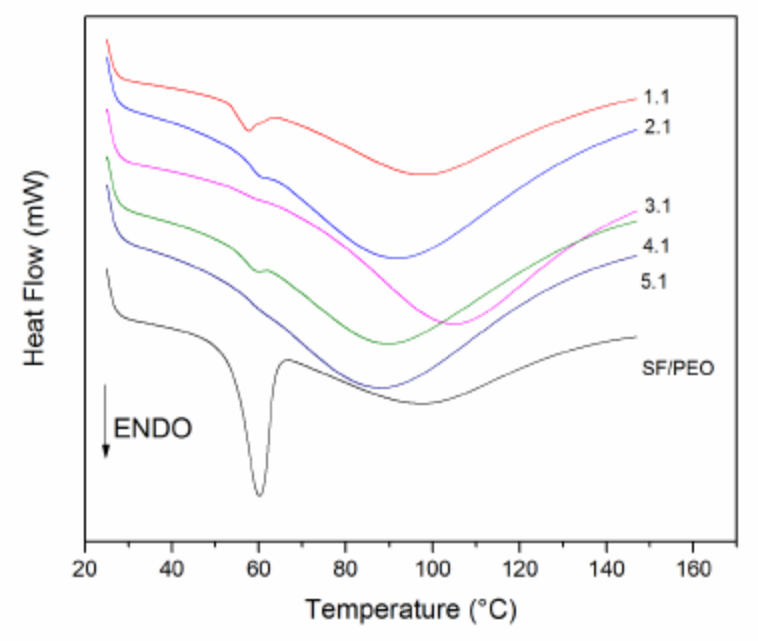

Figure 4

3.1.4 Energy dispersion X-ray spectroscopy (EDS).

Energy dispersion X-ray spectroscopy was used to obtain the chemical composition profile of the nanofibers. In this analysis, only nanofibers subjected to treatment with absolute ethanol at 60 °C were evaluated. All the samples were coated with thin film of carbon before EDS measurement, so the peak of C is universal. In the EDS spectra of samples 1.1, 2.1, and 5.1 (**Figure 5**) it is possible to observe peaks relative to SF (C, O, and N atoms), as well as a peak in the 2.25 - 2.50 eV range relative to CS and SSD (S atoms) and in the 2.90 - 3.25 eV range, relative to Ag. Thus, it can be stated that even after washing with absolute ethanol the CS and SSD remained in the nanofibers. EDS spectra of samples 3.1 and 4.1 display peaks concerning C, O, and N atoms of SF and also a peak in the 2.25 - 2.50 eV range relative to the S atoms. This indicates that even after the removal of PEO with absolute ethanol, CS remained in the nanofibers. However, it was not possible to observe the peak related to the presence of Ag in the 2.25 - 2.50 eV range, possibly due to the low SSD concentration used in these samples.

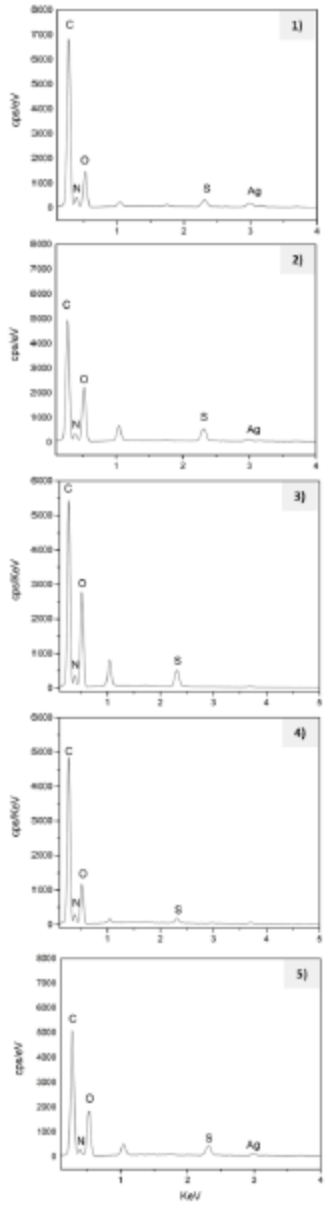

Figure 5

3.1.5 Flame atomic absorption spectrometry (FAAS).

Flame Atomic Absorption Spectrometry (AAS) analysis was used to verify the remaining SSD content in nanofibers after treatment with absolute ethanol to remove PEO. **Figure 6** compares the amount of Ag in the nanofibers before and after the treatment. Sample 1.1 showed almost 100% retention of the SSD in the nanofibers after washing with absolute ethanol, while 25% of SSD was washed out in sample 2.1. It suggests that SSD was better dispersed in sample 1.1 and, consequently, a higher fraction of SSD remained in such nanofibers. Similar results were found in samples 3.1 and 4.1, where the sample 4.1 presented around 100% of added SSD, while in sample 3.1 only 73%. It should be noted that the amounts of SSD added was higher in samples 1 and 2 (1.0%) and lower in samples 3 and 4 (0.1%); for CS the higher amounts were in samples 1 and 3 (5.0%) and lower in samples 2 and 4 (1.0%), while intermediate concentrations of SSD and CS were used in the formulation of sample 5 (0.5% and 3.0%, respectively) which presented 92% of the added SSD after the washing with ethanol.

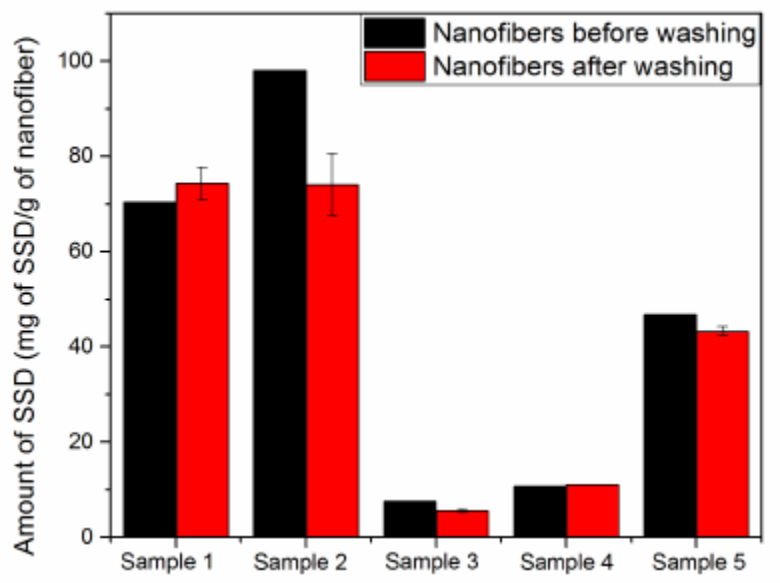

Figure 6

3.2 Biological assays of the nanofibers

3.2.1 Cytotoxicity

Cytotoxicity analysis was performed based on the observation of the cell viability of Vero cells, exposed to disks of the obtained nanofibers. If there is no reduction in cell viability in the presence of nanofibers, it can be assumed that nanofibers are non-toxic and, therefore, can be considered cytocompatible.

Three controls were used in this analysis. The first is the negative control, without the addition of nanofibers, and is, therefore, considered as a 100% reference. The second was the same aluminum foil (AF) where the samples were collected, to verify if the AF would affect the results in any way since it was not possible completely to separate it from the SF nanofibers samples; and the third was the as-collected SF nanofibers.

Through the analysis of Figure 7, it was possible to verify that all samples presented cell viability close to 100%, regardless the SSD and CS concentration used to obtain the nanofibers. The same cell viability was observed in the used controls. This result indicates that nanofibers are not toxic to Vero cells, as cell viability must be reduced by at least 30% to be considered cytotoxic (ISO document 10993-5 2009). So, the presence of CS in the scaffolds must compensate the toxicity of SSD, once the viability values were about 100% to all the samples, in reverse, Mina Mohseni et al.[38] showed that samples containing high concentrations of SSD were not able to support cell proliferation as well as the sample with the lower amount of Ag^{2+}, although, they empathize that the presence of fibronectin over the fibers may confer better cell attachment and growth. Comparing our work and Mohseni's, even though the studied cells were from different cultures, Vero vs fibroblast, the cellular mechanisms can be considered similar, once both are healthy cells from mammalian and are employed in several cytocompatibility assays. So, it is also worthy to affirm that our material behaved as positively responsive in front of a healthy cell line.

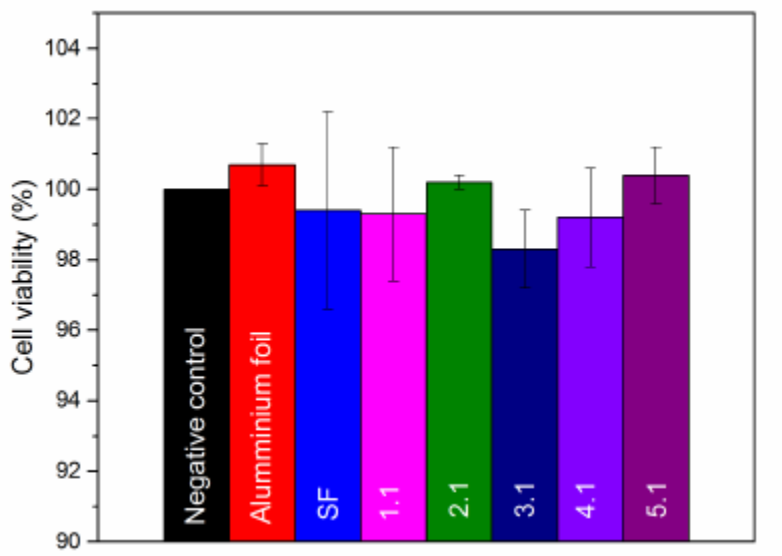

Figure 7

3.2.2 Antibacterial activity

Antibacterial activity analysis was used to verify the growth's inhibition of grampositive and gram-negative bacteria exposed to nanofiber discs. Three controls were used, the first was the AF, the second was the neat nanofibers (composed only by SF) and the third was nanofibers of SF / CS.

Figure 8 presents the obtained results. The controls AF, SF, and the SF / CS nanofibers showed no antibacterial activity, so they did not appear. For *S. aureus*, all samples containing SSD showed antibacterial activity, and the best results were obtained with samples containing the highest concentration (1.0%, m / v) of SSD (samples 1.1 and 2.1). Samples containing the lowest SSD concentration (0.1%, w / v) (samples 3.1 and 4.1) also showed antibacterial activity, but the inhibition zone was smaller, as did the sample containing the intermediate concentration (0.5%). w / v) SSD (sample 5.1). Antibacterial activity against *B. subtilis* was observed only in samples containing SSD concentration > 0.1% (samples 1.1, 2.1, and 5.1), being the best results obtained with samples 1.1 and 5.1, respectively. For *E. coli* and *P. aeruginosa*, only sample 4.1 showed no antibacterial activity. The best results for *E. coli* were obtained when the highest SSD concentration (1.0%, m / v) was used (samples 1.1 and 2.1) and for *P. aeruginosa*, the best results were found in nanofibers with concentrations of 1.0% and 0.5% SSD and 5.0% and 3.0% CS, respectively (samples 1.1 and 5.1).

Comparing the samples containing 1.0% SSD (samples 1.1 and 2.1) it was noted that when the concentration of CS was 5.0%, there was greater antibacterial activity compared to the concentration of 1.0% CS in *B. subtilis*, *E. coli*, and *P. aeruginosa*. For *S. aureus*, the antibacterial activity was practically the same, considering the standard deviation between replicates.

In samples with the lowest SSD concentration (0.1%, w/v) (samples 3.1 and 4.1), when the 5.0% (w/w) CS concentration was used, antibacterial activity was observed against three of the four bacteria analyzed, *S. aureus*, *E. coli*, and *P. aeruginosa*. The same did not occur when the concentration of CS was decreased to 1.0 (w/w) % and the concentration of SSD was kept at 0.1% (w/v), which shows that the CS positively influenced the antibacterial activity of nanofibers, which may be related to the interactions that are taking place between the CS and the SSD. On this case, SSD act most effectively against Gram-negative bacteria, for example, *P. aeruginosa* and *E. coli*, explained by the fact that besides Gram-negative

bacteria have a complex cell wall structure made by a layer of peptidoglycan and mats with barrier properties, Ag^{2+} ions interact preferable with that, instead of Gram-positive, which possess a cell wall composed by multilayered peptidoglycans [42]. In addition, beyond promoting a great index of cell viability, the presence of CS seems to confer a synergic effect to the antibacterial activity of SSD in the nanofibers forming considerable good inhibition zones (practically all samples upper then 10 mm), once when a material presents a value of 1 mm to the inhibition zone it is already considered as having a good bactericidal activity [43].
Sample 5.1, containing intermediate concentrations of SSD 0.5% (w/v) and CS 3.0% (w/w) also showed antibacterial activity against all tested bacteria.

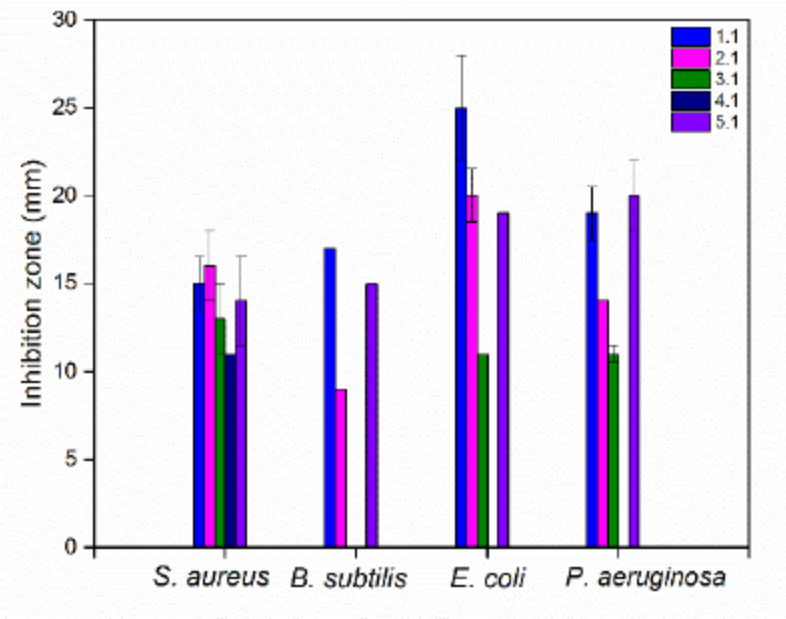

Figure 8

3.2.3 Histopathological evaluation in post-treatment to Wistar rats

In vivo biological activity analysis was used to verify the inhibition of growth of gram-positive and gram-negative bacteria in Wistar rats infected with *S. aureus* and *P. aeruginosa* exposed to nanofiber discs, as well as to evaluate wound healing time. The study was conducted with sample 5.1, as it presented excellent results both in the analysis of the remaining SSD content and *in vitro* antibacterial activity, especially against *S. aureus* and *P. aeruginosa* bacteria, which were the bacteria used in this study. The results are shown in **Figure 9**.
During the acute healing process, inflammatory cell infiltration ceases within few days after injury, whereas in infected wounds persistent levels of proinflammatory cytokines are reported and, in contrast, reduced levels of anti-inflammatory cytokines. In the process of chronic inflammation, the mechanical stability of the provisional matrix is diminished making it difficult to develop new blood vessels [44]. The transition from inflammatory to proliferative phase and granulation tissue formation is also considerably delayed [45].
It is observed that the animals of group G1 (uninfected and untreated) do not present, after 5 days, many inflammatory infiltrates (dark purple rounded cells) and that the healing process evolved (**Figure 9-A**). For the next stage, the proliferative phase, characterized by the formation of granulation tissue, this tissue has a pinkish color and the presence of fibroblasts (cells with a light purple color and a longer nucleus).
In groups G2 (infected with *S. aureus*) and G3 (infected with *P. aeruginosa*), there is still

many inflammatory infiltrates, indicating that there was a delay in the healing process caused by the infection (**Figure 9-B, C**).
In groups G4 and G5 (infected and treated with SSD cream) it is observed that there is a decrease in inflammatory infiltrates, showing that the SSD cream was effective in controlling the infection. It is also observed that the formation of granulation tissue has already started (characterized by the pinkest color) (**Figure 9-D, E**), as in G1. In groups G6 and G7 (infected and treated with SF nanofibers) there is a large number of inflammatory infiltrates (**Figure 9-F, G**), similar to that observed in animals of groups G2 and G3, confirming that SF did not affect bacteria growth, as already demonstrated *in vitro* tests.
In groups G8 and G9 (infected and treated with SF nanofibers containing CS and SSD) there is a great reduction in the number of inflammatory infiltrates and also the beginning of the formation of granulation tissue (**Figure 9-H, I**), similar to the results obtained in the groups G4 and G5 treated with SSD cream. Nevertheless, the result obtained is promising, since SSD cream was applied daily, which can cause discomfort and pain in the patient, while the treatment with SF nanofibers was performed only once, being more advantageous.
Yang Li et al.[46], presented a SSD charged spongy SF material applied as wound dressing in mice. After 5 days they had a good rate of regeneration with formation of granulation tissues and fibroblasts proliferation but, we consider our material of a better impact, once conditions applied in our *in vivo* assay implied rats infected with bacteria *P. aeruginosa* and *S. aureus* and presented the same rate of recovering. Comparison of results of this paper with ones of Yang Li et al.[46], it is clear that the presence of CS in the as-prepared SF nanofibers containing CS and SSD plays an important role in the effect of antibacterial of SSD.
Given the results presented, it was possible to conclude that the CS concentration influenced both the remaining SSD content in the nanofibers and the antibacterial activity presented by them. So, we did some preliminary tests to better understand how CS and SSD interact.

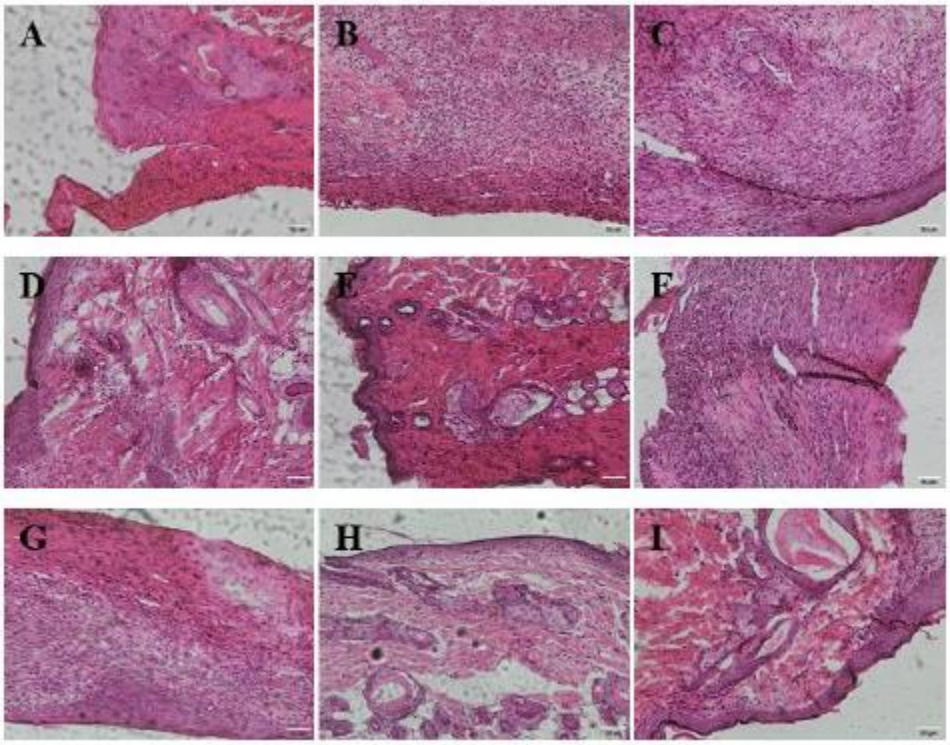

Figure 9

For this we prepared two solutions with the same amount of dispersed SSD, being the first dispersed at aqueous/HCl at pH = 1 and the second dispersed at aqueous pH = 1 containing 1.0-% CS (m / v), both after stirring for 24 hours and then left to rest for 24 hours. The result is presented in photos of **Figure 10**.
CS (which is anionic) acts, in this case, as a stabilizing agent in the medium, not allowing the SSD particles to agglomerate and improving its dispersion in the solution.
It was also obtained a film in the proportion (1: 1) of CS/SSD in water at pH 1.0 (same solvent used to obtain the spinning solutions) and then dried in an oven at 40 °C. This film was analyzed using DSC and FTIR-ATR techniques.

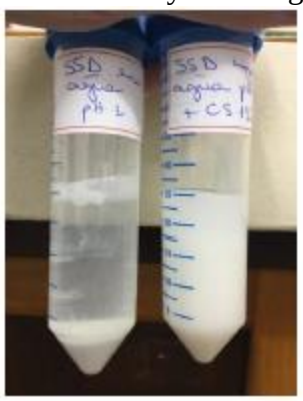

Figure 10
Figure 11 shows the DSC curves of the CS and as-obtained SSD film, the physical mixture of these materials, as well as the precursors. In the film, it was observed the displacement of the CS decomposition peak in comparison to the pure polymer, indicating that should have been interactions between CS and SSD. Analogous displacement was not observed when only the physical mixing of the materials is done. Another evidence of CS and SSD interactions is the disappearance of the SSD melting peak at 293 ° C on DSC curve for the film [47,48].

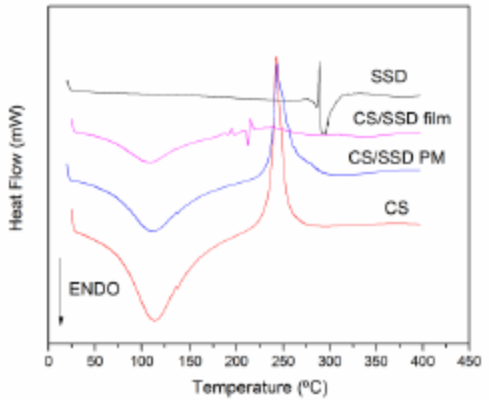

Figure 11
Figure 12 shows the FTIR-ATR spectra of the CS and SSD film obtained as well as the precursors. It was possible to notice the displacement of some bands of the precursors in the film spectrum, for the CS: 1030 to 1026 cm^{-1} and from 1228 to 1222 cm^{-1} and for the SSD: 1655 to 1730 cm^{-1}, 1500 to 1490 cm^{-1}, 1125 to 1150 cm^{-1}, 3345 to 3359 cm^{-1}, and 3390 to 3420 cm^{-1}. These displacements show once more the existence of interactions between CS and SSD and also with the Ag^{+} ions present in the solution. Thus, through the FTIR-ATR and DSC analyses of the as-obtained CS/SSD film, it was possible to verify that there are interactions between CS and SSD. However, further investigation is still needed to clarify the interactions that occur between these materials and how these interactions would contribute for the results obtained.

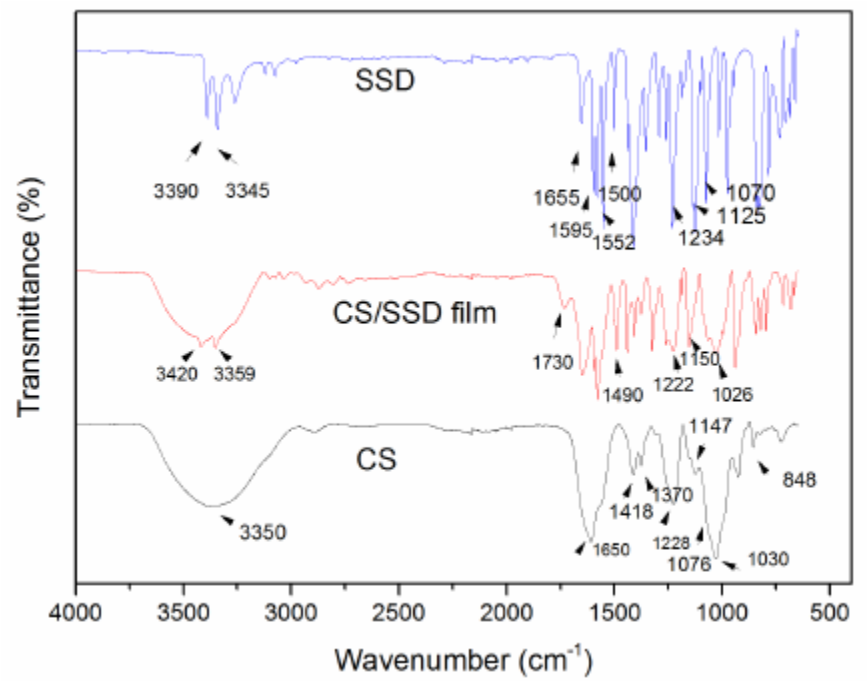

Figure 12

4. Conclusions

Nanofibers containing silk fibroin (SF), chondroitin sulfate (CS), and silver sulfadiazine **(**SSD) were obtained through electrospinning. The production of nanofibers containing such components intended to develop a new dressing [that has antibacterial activity and at the same time good characteristics for skin regeneration] to treat burns and skin wounds. Images obtained by SEM showed that the nanofibers have homogeneous morphology. As demonstrated by FTIR-ATR and DSC analysis, the PEO increased the poor electrospinnability (due to the low viscosity of the SF solution) and it was superficially removed from the nanofibers using absolute ethanol. Besides, FTIR spectra indicated that CS remained in the nanofibers after the absolute ethanol treatment, possibly due to hydrogen bonds with SF. The results of the EDS analysis showed that after partial removal of PEO, the SSD remained in the nanofibers. Quantification of Ag^{+} ions on the surface of the nanofibers showed that CS had a major influence on the remaining SSD, possibly due to the interaction CS-Ag^{+} and also CS-SSD present in the solution, forming a polyelectrolytic complex, which favored the permanence of SSD in the nanofibers. Biological assays proved that nanofibers were non-toxic against Vero cells and showed antibacterial activity. The best results were obtained using SSD concentrations (w/v) of 1.00% and 0.55% and concentrations (w/w) 5.00% and 3.00% of CS. Antibacterial activity trials also exhibited that CS concentration had a major influence on antibacterial activity. *In vivo* experiments indicated that SF nanofibers composed of CS and SSD presented results like standard SSD cream treatment, but with the advantage of being applied only once to the patient avoiding discomfort and pain in dressing change and reapplication of treatment as occurs with conventional SSD cream. FTIR-ATR and DSC analyzes of the CS / SSD film confirmed that the CS and the sulfadiazine interact with each other and that it may be due to this that the SSD shows better dispersion in the presence of the CS. The material produced in this work presents a great capability to be applied as a wound dressing to assist wound damaged tissues, mainly occasioned by burning.

Author Contributions
Marília Cestari: Conceptualization, Methodology, Writing the draft.
Bárbara Sthéfani Caldas: Methodology, Review & Editing.
Dyenefer Pereira Fonseca: Methodology.
Rodolfo Bento Balbinot: Methodology.
Danielle Lazarin-Bidóia: Methodology.
Issei Otsuka: Methodology, Review & Editing.
Celso Vataru Nakamura: Investigation.
Redouane Borsali: Investigation, Writing - Review & Editing.
Edvani Curti Muniz: Supervision, Writing - Review & Editing.

Conflicts of interest
Authors declare that there is no conflict of interest of any type, in this work, neither that the financial support for this work has been influenced our findings.

Acknowledgements
Authors would like to acknowledge the institutions that sponsored this work, CNPq - Conselho Nacional de Desenvolvimento Científico e Tecnológico (Grant 423818/2018-0, 400702/2012-6, and #307429/2018-0) and CAPES – Coordenação de Aperfeiçoamento de Pessoal de Nível Superior and BioRender.com by illustration tools.

Notes and references
[1] L.A. Barajas-Nava, J. López-Alcalde, M.R. i Figuls, I. Solà, X.B. Cosp, Antibiotic prophylaxis for preventing burn wound infection (Review), Cochrane Database Syst. Rev. (2013). https://doi.org/10.1002/14651858.CD008738.pub2.www.cochranelibrary.com.
[2] D. Church, S. Elsayed, O. Reid, B. Winston, R. Lindsay, Burn Wound Infections, Clin. Microbiol. Rev. 19 (2006) 403–434. https://doi.org/10.1128/CMR.19.2.403.
[3] R. Edwards, K.G. Harding, Bacteria and wound healing Colonisation Contamination, Curr. Opin. Infect. Dis. (2004) 91–96. https://doi.org/10.1097/01.qco.0000124361.27345.d4.
[4] A.J. Singer, S.A. McClain, Persistent wound infection delays epidermal maturation and increases scarring in thermal burns, Wound Repair Regen. 10 (2002) 372–377. https://doi.org/10.1046/j.1524-475X.2002.10606.x.
[5] J.S. Boateng, K.H. Matthews, H.N.E. Stevens, G.M. Eccleston, Wound healing dressings and drug delivery systems: a review., J. Pharm. Sci. 97 (2008) 2892–2923. https://doi.org/10.1002/jps.21210.
[6] M. Maaz Arif, S.M. Khan, N. Gull, T.A. Tabish, S. Zia, R. Ullah Khan, S.M. Awais, M. Arif Butt, Polymer-based biomaterials for chronic wound management: Promises and challenges, Int. J. Pharm. 598 (2021) 120270. https://doi.org/https://doi.org/10.1016/j.ijpharm.2021.120270.
[7] G.D. Mogoşanu, A.M. Grumezescu, Natural and synthetic polymers for wounds and burns dressing, Int. J. Pharm. 463 (2014) 127–136. https://doi.org/https://doi.org/10.1016/j.ijpharm.2013.12.015.
[8] S. Templer, M. Brito, Bacterial Skin and Soft Tissue Infections, Curr. Opin. Infect. Dis. - CURR OPIN INFECT DIS. 5 (2009).
[9] O. Sarheed, Antimicrobial Dressings for Improving Wound Healing, in: A. Ahmed (Org.), IntechOpen, Rijeka, 2016: p. Ch. 17. https://doi.org/10.5772/63961.
[10] A.F. Cardona, S.E. Wilson, Skin and soft-tissue infections: a critical review and the role of telavancin in their treatment., Clin. Infect. Dis. an Off. Publ. Infect.

Dis. Soc. Am. 61 Suppl 2 (2015) S69-78. https://doi.org/10.1093/cid/civ528.
[11] N. Woodford, D.M. Livermore, Infections caused by Gram-positive bacteria: a review of the global challenge., J. Infect. 59 Suppl 1 (2009) S4-16. https://doi.org/10.1016/S0163-4453(09)60003-7.
[12] G.D. WINTER, Formation of the Scab and the Rate of Epithelization of Superficial Wounds in the Skin of the Young Domestic Pig, Nature. 193 (1962) 293–294. https://doi.org/10.1038/193293a0.
[13] M. Abrigo, S.L. McArthur, P. Kingshott, Electrospun nanofibers as dressings for chronic wound care: advances, challenges, and future prospects., Macromol. Biosci. 14 (2014) 772–792. https://doi.org/10.1002/mabi.201300561.
[14] R.S. Ambekar, B. Kandasubramanian, Advancements in nanofibers for wound dressing: A review, Eur. Polym. J. 117 (2019) 304–336. https://doi.org/https://doi.org/10.1016/j.eurpolymj.2019.05.020.
[15] M.Á.R. Calderón, W. Zhao, Applications of Polymer Nanofibers in Bio-Materials, Biotechnology and Biomedicine: A Review BT - TMS 2014: 143rd Annual Meeting & Exhibition, in: Springer International Publishing, Cham, 2016: p. 401–414.
[16] S.R. Bhattarai, N. Bhattarai, H.K. Yi, P.H. Hwang, D. Il Cha, H.Y. Kim, Novel biodegradable electrospun membrane: scaffold for tissue engineering., Biomaterials. 25 (2004) 2595–2602. https://doi.org/10.1016/j.biomaterials.2003.09.043.
[17] P. Zahedi, I. Rezaeian, S.-O. Ranaei-Siadat, S.-H. Jafari, P. Supaphol, A review on wound dressings with an emphasis on electrospun nanofibrous polymeric bandages, Polym. Adv. Technol. 21 (2010) 77–95. https://doi.org/https://doi.org/10.1002/pat.1625.
[18] A.R. Fajardo, L.C. Lopes, A.O. Caleare, E. a. Britta, C. V. Nakamura, A.F. Rubira, E.C. Muniz, Silver sulfadiazine loaded chitosan/chondroitin sulfate films for a potential wound dressing application, Mater. Sci. Eng. C. 33 (2013) 588–595. https://doi.org/10.1016/j.msec.2012.09.025.
[19] P.A. Howard, L.C. Cancio, A.T. McManus, C.W. Goodwin, S.H. Kim, B.A. Pruitt, What's new in burn-associated infections?11The views expressed in this article are the private opinions of the authors and do not necessarily reflect the official views of the Department of the Army or Department of Defense., Curr. Surg. 56 (1999) 397–405. https://doi.org/https://doi.org/10.1016/S0149-7944(99)00166-X.
[20] K. Ito, A. Saito, T. Fujie, K. Nishiwaki, H. Miyazaki, M. Kinoshita, D. Saitoh, S. Ohtsubo, S. Takeoka, Sustainable antimicrobial effect of silver sulfadiazine-loaded nanosheets on infection in a mouse model of partial-thickness burn injury., Acta Biomater. 24 (2015) 87–95. https://doi.org/10.1016/j.actbio.2015.05.035.
[21] C. Vepari, D.L. Kaplan, Silk as a Biomaterial., Prog. Polym. Sci. 32 (2007) 991–1007. https://doi.org/10.1016/j.progpolymsci.2007.05.013.
[22] C. Zhao, T. Asakura, Structure of Silk studied with NMR, Prog. Nucl. Magn. Reson. Spectrosc. 39 (2001) 301–352. https://doi.org/https://doi.org/10.1016/S0079-6565(01)00039-5.
[23] E. Wenk, H.P. Merkle, L. Meinel, Silk fibroin as a vehicle for drug delivery applications, J. Control. Release. 150 (2011) 128–141. https://doi.org/10.1016/j.jconrel.2010.11.007.
[24] L. Jeong, M.H. Kim, J.-Y. Jung, B.M. Min, W.H. Park, Effect of silk fibroin nanofibers containing silver sulfadiazine on wound healing., Int. J. Nanomedicine. 9 (2014) 5277–87. https://doi.org/10.2147/IJN.S71295.
[25] S. Yan, Q. Zhang, J. Wang, Y. Liu, S. Lu, M. Li, D.L. Kaplan, Silk

fibroin/chondroitin sulfate/hyaluronic acid ternary scaffolds for dermal tissue reconstruction, Acta Biomater. 9 (2013) 6771–6782. https://doi.org/10.1016/j.actbio.2013.02.016.
[26] M.E. Gilbert, K.R. Kirker, S.D. Gray, P.D. Ward, J.G. Szakacs, G.D. Prestwich, R.R. Orlandi, O. Hypothesis, Chondroitin Sulfate Hydrogel and Wound Healing in Rabbit Maxillary Sinus Mucosa, Laryngoscope. 114 (2004) 1406–1409.
[27] X.H. Zou, Y.Z. Jiang, G.R. Zhang, H.M. Jin, N.T.M. Hieu, H.W. Ouyang, Specific interactions between human fibroblasts and particular chondroitin sulfate molecules for wound healing, Acta Biomater. 5 (2009) 1588–1595. https://doi.org/10.1016/j.actbio.2008.12.001.
[28] X. Wang, B. Ding, G. Sun, M. Wang, J. Yu, Electro-spinning/netting: A strategy for the fabrication of three-dimensional polymer nano-fiber/nets, Prog. Mater. Sci. 58 (2013) 1173–1243. https://doi.org/10.1016/j.pmatsci.2013.05.001.
[29] Y.M. Iyaguchi, H.U. Jianen, Technical paper Physicochemical Properties of Silk Fibroin after Solubilization Using Calcium Chloride with or without Ethanol, Food Sci. Technol. Res. 11 (2005) 37–42. https://doi.org/10.3136/fstr.11.37.
[30] X. Zhang, C.B. Baughman, D.L. Kaplan, In vitro evaluation of electrospun silk fibroin scaffolds for vascular cell growth, Biomaterials. 29 (2008) 2217–2227. https://doi.org/10.1016/j.biomaterials.2008.01.022.
[31] M. Cestari, V. Muller, J.H.D.S. Rodrigues, C.V. Nakamura, A.F. Rubira, E.C. Muniz, Preparing silk fibroin nanofibers through electrospinning: Further heparin immobilization toward hemocompatibility improvement, Biomacromolecules. 15 (2014). https://doi.org/10.1021/bm500132g.
[32] J. Chutipakdeevong, U.R. Ruktanonchai, P. Supaphol, Process optimization of electrospun silk fibroin fiber mat for accelerated wound healing, J. Appl. Polym. Sci. 130 (2013) 3634–3644. https://doi.org/10.1002/app.39611.
[33] T. Higuchi, N. Pilpel, T. Actual, C. Area, B. Touching, C. Bureau, N. York, C. Yip, D. Train, I. Pharmacy, S. Leigh, E. Carless, W. Burt, N. York, A.R. December, T.U. Company, H. Ballen, C.C. Sperry, Solubility Studies of Silver Sulfadiazine, 66 (1977) 519–522.
[34] X. Wen, Y. Zheng, J. Wu, L. Yue, C. Wang, J. Luan, Z. Wu, In vitro and in vivo investigation of bacterial cellulose dressing containing uniform silver sulfadiazine nanoparticles for burn wound healing, Prog. Nat. Sci. Mater. Int. 25 (2015) 197–203. https://doi.org/10.1016/j.pnsc.2015.05.004.
[35] T. Mosmann, Rapid Colorimetric Assay for Cellular Growth and Survival : Application to Proliferation and Cytotoxicity Assays, 65 (1983) 55–63.
[36] M. Balouiri, M. Sadiki, S.K. Ibnsouda, Methods for in vitro evaluating antimicrobial activity: A review, J. Pharm. Anal. 6 (2016) 71–79. https://doi.org/https://doi.org/10.1016/j.jpha.2015.11.005.
[37] N.R. Bhalodia, V.J. Shukla, Antibacterial and antifungal activities from leaf extracts of Cassia fistula l .: An ethnomedicinal plant, 2 (2011) 104–109. https://doi.org/10.4103/2231-4040.82956.
[38] M. Mohseni, A. Shamloo, Z. Aghababaei, M. Vossoughi, H. Moravvej, Antimicrobial Wound Dressing Containing Silver Sulfadiazine With High Biocompatibility: In Vitro Study, Artif. Organs. 40 (2016) 765–773. https://doi.org/https://doi.org/10.1111/aor.12682.
[39] S. De-bing, D. Zhi-hui, F. Wei-guo, Study on the Properties of the Electrospun Silk Fibroin / Gelatin Blend Nanofibers for Scaffolds, (2008). https://doi.org/10.1002/app.
[40] Q. Lu, B. Zhang, M. Li, B. Zuo, D.L. Kaplan, Y. Huang, H. Zhu, Degradation

Mechanism and Control of Silk Fibroin, (2011) 1080–1086. https://doi.org/10.1021/bm101422j.
[41] Z. Song, S.W. Chiang, X. Chu, H. Du, J. Li, L. Gan, C. Xu, Y. Yao, Y. He, B. Li, F. Kang, Effects of solvent on structures and properties of electrospun poly(ethylene oxide) nanofibers, J. Appl. Polym. Sci. 135 (2018) 45787. https://doi.org/https://doi.org/10.1002/app.45787.
[42] S. Ahmadian, M. Ghorbani, F. Mahmoodzadeh, Silver sulfadiazine-loaded electrospun ethyl cellulose/polylactic acid/collagen nanofibrous mats with antibacterial properties for wound healing., Int. J. Biol. Macromol. 162 (2020) 1555–1565. https://doi.org/10.1016/j.ijbiomac.2020.08.059.
[43] T. Baygar, Characterization of silk sutures coated with propolis and biogenic silver nanoparticles (AgNPs); an eco-friendly solution with wound healing potential against surgical site infections (SSIs), Turkish J. Med. Sci. 50 (2020) 258–266. https://doi.org/10.3906/sag-1906-48.
[44] A.G. Arroyo, M.L. Iruela-Arispe, Extracellular matrix, inflammation, and the angiogenic response, Cardiovasc. Res. 86 (2010) 226–235. https://doi.org/10.1093/cvr/cvq049.
[45] M. Aberg, U. Hedner, S. Jacobsson, U. Rothman, Fibrinolytic activity in wound secretions., Scand. J. Plast. Reconstr. Surg. 10 (1976) 103–105.
[46] Y. Li, X. Zha, X. Jiang, X. Yan, Z. Ying, F. Haojiang, X. Linqing, Z. Qifeng, A Promising Wound Dressing from Regenerated Silk Fibroin Sponge with Sustained Release of Silver Nanoparticles, J. Renew. Mater. 9 (2021) 295–310. https://doi.org/10.32604/jrm.2021.012271.
[47] M. Naeimi, M. Fathi, M. Rafienia, S. Bonakdar, Silk Fibroin-Chondroitin Sulfate-Alginate Porous Scaffolds : Structural Properties and In Vitro Studies, J. Appl. Polym. Sci. 41048 (2014) 1–9. https://doi.org/10.1002/app.41048.
[48] G. Sandri, M.C. Bonferoni, F. Ferrari, S. Rossi, C. Aguzzi, M. Mori, P. Grisoli, P. Cerezo, M. Tenci, C. Viseras, C. Caramella, Montmorillonite-chitosan-silver sulfadiazine nanocomposites for topical treatment of chronic skin lesions: In vitro biocompatibility, antibacterial efficacy and gap closure cell motility properties, Carbohydr. Polym. 102 (2014) 970–977. https://doi.org/10.1016/j.carbpol.2013.10.029.

Figure captions

Figure 1. SEM images of SF / PEO / CS / SSD nanofibers obtained at different concentrations before (left) and after (right) PEO removal with absolute ethanol.
Figure 2. Average diameter of nanofibers obtained before (blue) and after (red) PEO removal
Figure 3. FTIR-ATR spectra of the nanofibers (samples 1, 2, 3, 4, and 5). Comparison between a) before (red line) and b) after PEO removal (black line).
Figure 4. DSC curves of the as-obtained nanofibers after treatment with absolute ethanol for PEO removal (samples 1.1 to 5.1).
Figure 5. EDS spectra of the samples (1.1, 2.1, 3.1, 4.1, and 5.1) after PEO removal.
Figure 6. Relation between amounts of SSD added in nanofibers (samples 1.to 5), i.e., before treatment with absolute ethanol to remove PEO (black); and SSD remaining after ethanol treatment (red).
Figure 7. Cell viability assays in Vero cells exposed to the controls (negative control, AF and SF), and nanofibers disks containing SF, CS, and SSD after PEO removal.
Figure 8. Antibacterial activity of SF nanofibers, containing CS and SSD obtained after removal of PEO, exposed to gram-positive and gram-negative bacteria.

Figure 9. Histological analysis of skin of Wistar rats after 5 days of treatment with nanofibers. (A) G1 group: uninfected and untreated. (B) G2 group: infected with *S. aureus* and untreated. (C) G3 group: infected with *P. aeruginosa* and untreated. (D) G4 group: infected with *S. aureus* and treated with SSD cream. (E) G5 group: infected with *P. aeruginosa* and treated with SSD cream. (F) G6 group: infected with *S. aureus* and treated with nanofibers from SF. (G) G7 group: infected with *P. aeruginosa* and treated with nanofibers from SF. (H) G8 group: infected with *S. aureus* and treated SF nanofibers containing CS and SSD. (I) G9 group: infected with *P. aeruginosa* and treated SF nanofibers containing CS and SSD.

Figure 10. Comparison between the dispersion of SSD in water pH 1.0 (left) and in CS 1.0% solution (m / v) (right), at pH 1.0.

Figure 11. DSC curves of the CS / SSD film obtained, the physical mixture between CS and SSD, and the pure precursors.

Figure 12. FTIR-ATR spectra of the obtained CS / SSD film and precursors.

Figure